CCD Photometry in *VRI* Bands of the Galactic Cluster NGC 2818*

R. Surendiranath, N. Kameswara Rao, Ram Sagar, J. S. Nathan &
K. K. Ghosh *Indian Institute of Astrophysics, Bangalore 560034*

Abstract. The open cluster NGC 2818 containing a planetary nebula has been observed in *VRI* bands using the CCD system at prime focus of the 2.3-metre Vainu Bappu Telescope. The study extending to stars $V \sim 21$ magnitude establishes the distance modulus as $(m - M)_0 = 12.9 \pm 0.1$ for the cluster. Based on the fitting of theoretical isochrones computed for solar metallicity, an age of $5(\pm1) \times 10^8$ years has been assigned to the cluster. Association of the planetary nebula with the cluster indicates that the progenitor mass of the planetary nebula on the main sequence is $\geq 2.5 M_\odot$.

Key words: open clusters—*VRI* photometry—planetary nebulae—stellar evolution—open clusters, individual: NGC 2818

1. Introduction

NGC 2818 (C 0914-364) has the unique distinction of being one of the two galactic clusters associated with a planetary nebula (PN) also designated as NGC 2818 (= PK 261 + 8º1). An accurate estimate of the distance to the cluster gives us an opportunity to determine the size as well as the mass of the progenitor of the planetary nebula. Tifft, Connolly & Webb (1972; hereafter denoted as TCW) have presented *UBV* photographic photometry up to a limiting magnitude of $V \simeq 16.8$ and estimated the reddening and the distance to the cluster as $E(B - V) \simeq 0.22$ and 3.2 kpc respectively. According to TCW the cluster radial velocity of $+ 3 \pm 20$ km s^{-1} agrees with that of the PN $+ 8 \pm 13$ km s^{-1}. The reddening of the nebula estimated as $E(B - V) = 0.24$ is roughly the same as that of the cluster. However there seems to be a discrepancy in the estimated distance of the nebula and the cluster. Various statistical methods of estimating the distance of the PN range from 1.61 to 2.64 kpc (Kohoutek, Roth-Hopper & Lausten 1986) whereas estimates of the cluster distance range from 3.5 to 3.8 kpc (Dufour 1984). The estimate of the cluster distance modulus by TCW was based on main-sequence stars located in a narrow range of magnitude between the limit of their photometry (V ~ 16.8) and the turnoff point ($V \sim 16$) which gave little scope for a good zero age main sequence fitting for estimating the distance modulus. Thus to have a better estimate of the distance modulus it is necessary to extend the photometry deeper at least to $V \sim 19$ to 20 magnitude, and as such we have observed

---

this cluster with the 2.3-metre Vainu Bappu Telescope (VBT) with the main aim of estimating a better distance modulus.

2. Data

2.1 *Observations*

The observations in *VRI* filters (*R* and *I* in Cousins system) have been obtained with the CCD system described by Ananth *et al.* (1989) operating at the prime focus of the 2.3-m VBT. In brief, the CCD camera consists of a GEC P8603 chip with 512 × 320 pixels with a pixel size of 22 μm and operated through a PC/AT system. At the prime focus of the telescope a pixel of the CCD camera corresponds to ~ 0.6 arcsec on the sky and the entire camera covers a field of 5 × 3 arcmin^2. Observations of three fields of the cluster shown in Fig. 1 (primarily the zone 1 of TCW) have been obtained during 1989 April 3–5 in the three filters *V, R* and *I*. The evening and morning twilight sky was used for the flat field corrections. The details of the exposures are given in Table 1. Along
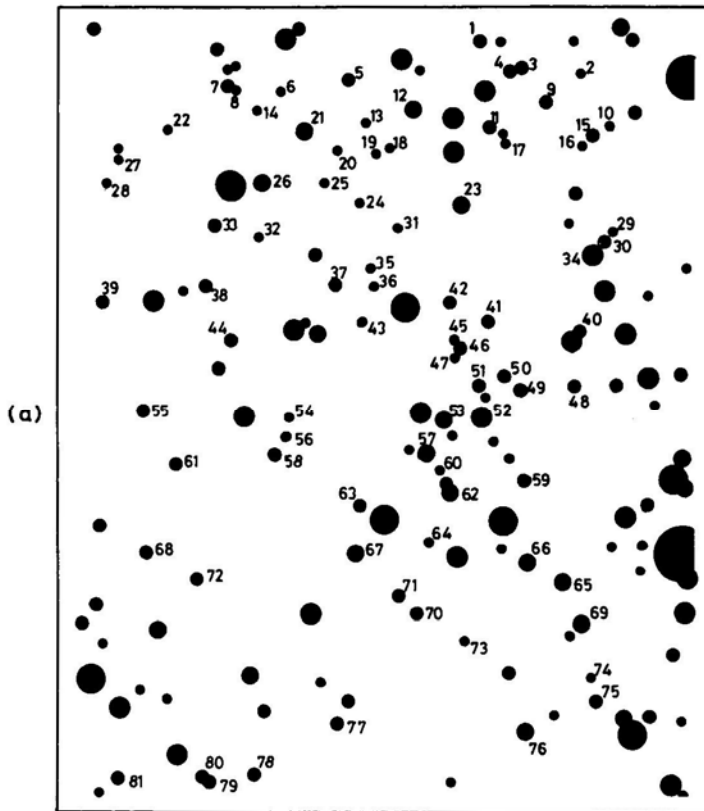

Figure 1. The observed CCD fields of the cluster NGC 2818; the numbers beside the stars correspond to Table 2. (a) Centred around star # 2–65 of TCW. α, δ(1950): 9^h 13^m 48^{s}4, – 36°24'37.0" (b) Centred around star # 1–89 of TCW. The star shown by an open circle may be a variable. (c) Right: centred around star # 1–167 of TCW.
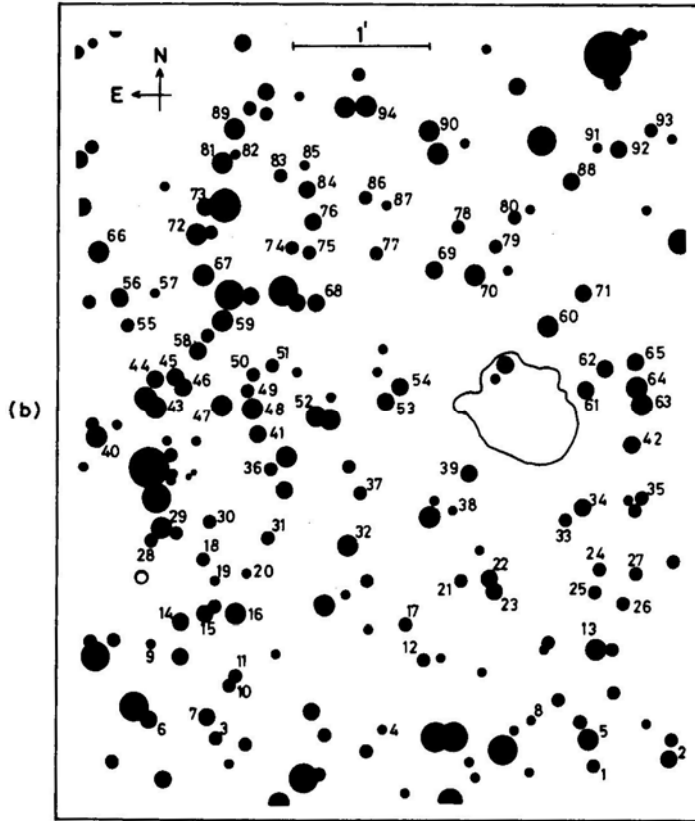
Figure 1. Continued.

with the cluster fields, standards located in clusters NGC 4147 and M 92 (Christian *et al.* 1985) have also been observed on these nights for calibration.

2.2 *Reductions*

The reductions of the CCD images were done using the STARLINK and STARMAN programs devised for stellar photometry (Penny 1987), using the VAX 11/780 system at Vainu Bappu Observatory. The magnitude estimation of stars on each of the data frames has been done by an iterative least squares fitting using the modified Lorentzian profile introduced by Penny & Dickens (1986) to account for the wide halo around stars. It is a rotated-elliptical Lorentzian with a wide low circular modified Gaussian base. The profile parameters were estimated for each frame using several bright (good S/N ratio) and isolated stars in the frame. Display and interaction with the image frames were done outside the STARLINK package, using the software developed locally for the COMTAL vision/1 image display station. About 400 stellar images have been measured in each filter. The pixel to pixel variation of the flat field frames was less than ~ 10 per cent. The mean atmospheric extinction coefficients for the site have been used to correct the instrumental magnitudes for atmospheric extinction. The colour
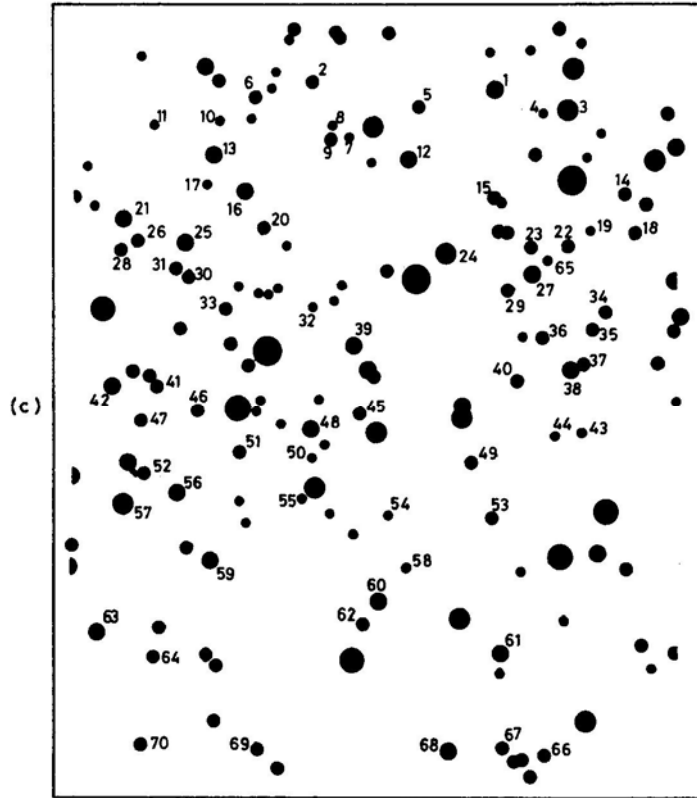
Figure 1. Continued.

and magnitudes were transformed using linear equations which were found to be adequate.

The equations used were

$$V = C_5 + C_6(V - I) + v_i,$$

$$(V - I) = C_1(v - i)_i + C_2,$$

$$(V - R) = C_3(v - r)_i + C_4.$$

The rms error in each of these fits was 0.06 mag. The magnitude and colour range covered by the standards are V = 15.9 to 18.3, $V - I$ = − 0.09 to 1.44, and $V - R$ = − 0.09 to 0.71. The standards used (Christian a al. 1985) for transformation themselves have residuals of this order: 0.05 in $(V - I)$ and 0.025 in $(V - R)$. Since we do not have local standards for R and I magnitudes, we checked these transformations using the standards in the following way: for stars which occur on the cluster main-sequence in the $V/(B - V)$ diagram of TCW (*i.e.* Fig. 2 of TCW, V = 14.8 to 15.7 and $B - V$ = 0.22 to 0.40) we applied the cluster reddening corrections (see Section 3.1 for the relations used) to estimate the expected $V - R$ and $V - I$ colours using the intrinsic colours for dwarfs as given by Bessell (1979). These values agree with direct transformations within ±0.05 and ±0.04 magnitudes in $V - I$ and $V - R$ colours respectively. The zero points of the colours have been checked thus and the V magnitude zero point was

Table 1. Log of observations.

Date (1989)	Filter	Exp. time (s)	Field covered
April 3	V	720	Fig. 1(b)
	R	120	,,
	I	60	,,
	V	600	M 92
	R	420	,,
	I	300	,,
	V	600	N 4147
	R	300	,,
	I	480	,,
April 5	V	1200	Fig. 1(a)
	R	240	,,
	I	360	,,
	V	1200	Fig. 1(c)
	R	240	,,
	I	360	,,
	V	1200	N 4147
	R	240	,,
	I	360	,,
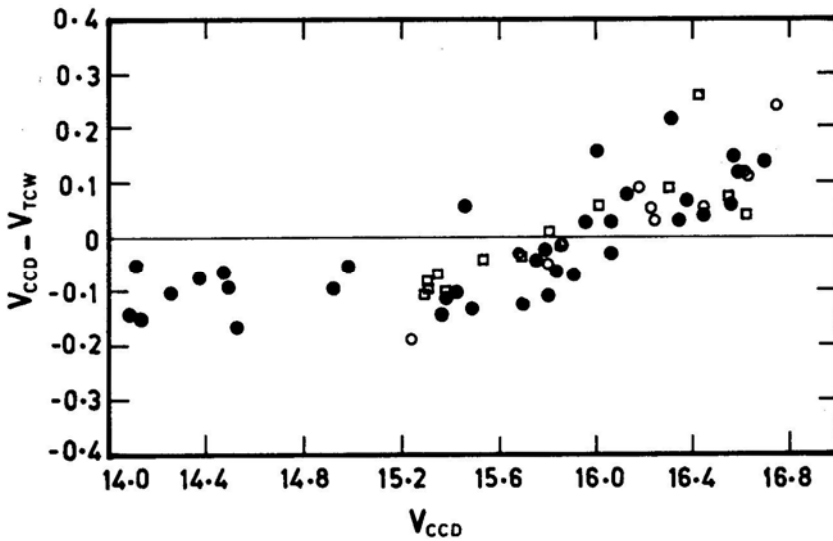
Figure 2. The difference of V magnitudes of this study and of TCW ($V_{CCD} - V_{TCW}$) plotted with respect to the V magnitudes of this study (V_{CCD}).

checked with that of TCW stars. The internal errors in V, $V–R$ and $V–I$ (*i.e.* for the same stars from different frames) are $\pm$ 0.035, $\pm$ 0.02 respectively. The V, $V–I$ and $V–R$ values are tabulated in Table 2, along with cross identification with TCW. These star numbers correspond to the numbers given in Fig. 1.

The comparison with TCW's V magnitudes is shown in Fig. 2. The TCW magnitudes are based on photographic photometry and are claimed to be accurate to

R. Surendiranath et al.

Table 2. Photometric results on NGC 2818.

Fig. 1(a) No.	TCW No.	V	$V-R$	$V-I$
1		20.62	3.87	4.75
2		19.46	0.97	1.64
3		16.99	0.62	1.31
4		17.49	0.53	0.62
5		18.07	0.81	1.51
6		19.62	1.75	3.12
7		16.95	0.45	0.82
8		18.63	0.26	0.74
9		17.69	0.78	1.42
10		18.98	0.67	1.12
11		17.52	0.34	0.62
12		16.99	0.42	0.76
13		18.22	0.43	0.77
14		18.65	0.67	1.27
15		17.81	0.60	1.06
16		18.77	0.64	1.03
17		18.44	0.67	1.15
18		18.65	0.71	1.37
19		18.70	0.46	0.85
20		18.36	0.48	0.93
21		16.51	0.44	0.83
22		18.03	0.90	1.63
23	1–13	15.29	0.21	0.45
24		19.77	1.02	1.92
25		19.21	0.15	0.50
26	2–134	15.69	0.31	0.58
27		18.18	0.50	1.05
28		18.98	0.28	0.23
29		19.09	0.91	1.56
30		17.59	1.14	2.04
31		18.34	0.43	0.82
32		18.66	−0.07	0.15
33	2–136	16.30	0.35	0.65
34	1–17	15.38	0.24	0.50
35		18.00	0.43	0.85
36		18.45	0.29	0.32
37	1–14	16.62	0.41	0.76
38		17.51	0.50	0.85
39		18.02	0.66	1.27
40		19.12	0.38	0.97
41		18.33	0.91	1.57
42		17.14	0.60	1.03
43		18.29	0.40	0.76
44		18.44	0.60	1.31
45		19.32	1.29	2.35
46		17.04	0.64	1.16
47		18.72	0.64	1.12
48		17.18	0.47	0.87
49		17.95	0.51	0.88
50		18.63	0.72	1.23
51		17.44	0.58	1.04
52	1–169	15.31	0.19	0.41

Table 2. Continued.

Fig. 1(a) No.	TCW No.	V	V − R	V − I
53	1–168	16.58	0.50	0.91
54		19.37	0.95	1.66
55		18.39	0.65	1.34
56		17.81	0.70	1.27
57	1–163	15.81	0.33	0.63
58	1–164	16.55	0.36	0.69
59	1–162	16.42	0.68	1.19
60		19.34	0.74	1.13
61		18.12	0.82	1.50
62	1–160	16.44	0.48	0.85
63		17.50	0.47	0.87
64		18.68	0.00	−0.01
65	1–149	15.35	0.25	0.52
66	1–150	15.53	0.31	0.60
67	1–157	16.01	0.46	0.86
68		17.13	0.62	1.22
69	1–148	15.31	0.19	0.41
70		16.74	0.42	0.78
71		17.90	0.50	0.94
72		17.42	0.45	0.87
73		18.52	0.43	0.70
74		19.63	0.65	1.36
75		17.83	0.54	1.00
76	1–152	15.16	0.12	0.30
77		18.13	0.71	1.29
78		16.85	0.42	0.89
79		18.08	1.13	1.56
80		16.91	−0.12	1.16
81		17.02	0.37	1.10

Fig. 1(b) No.	TCW No.	V	V − R	V − I
1		17.79	0.40	0.64
2		16.14	0.23	0.53
3		17.57	0.39	0.80
4		18.99	0.43	0.88
5	2–48	14.09	—	0.24
6	1–134	16.31	0.22	0.70
7	1–136	15.84	0.28	0.58
8		18.25	0.41	0.93
9		18.56	0.03	0.41
10		17.40	0.30	0.48
11		19.36	0.60	1.74
12	1–123	16.78	0.30	0.59
13	1–100	14.13	—	0.29
14		17.37	0.56	1.09
15	1–140	15.48	0.19	0.46
16	1–138	14.37	—	0.50
17		19.16	0.88	1.94
18		18.06	0.43	0.77
19		19.42	0.70	1.46
20		18.56	0.11	0.10

Table 2.   Continued.

Fig. 1(b) No.	TCW No.	V	V − R	V − I
21		18.73	0.57	0.77
22	1–103	16.34	0.29	0.56
23	1–102	15.70	0.16	0.41
24		16.96	0.40	0.77
25	1–97	15.76	0.43	0.85
26	1–98	16.32	0.13	0.46
27		18.63	0.77	1.05
28		18.34	0.40	0.73
29		16.33	0.48	0.99
30		17.05	0.39	0.75
31		20.74	1.65	2.99
32	1–121	14.52	—	0.14
33	1–95	16.57	0.29	0.86
34	1–94	15.24	0.10	0.28
35		16.78	0.46	0.97
36		17.51	0.55	0.83
37		17.53	0.51	0.92
38		18.78	0.49	0.70
39		17.23	0.50	0.95
40	1–144	14.25	—	0.32
41	1–117	16.13	0.37	0.71
42	1–81	16.44	0.29	0.59
43	1–114	15.15	0.21	0.48
44	1–112	16.06	0.30	0.69
45	1–111	16.55	0.29	0.56
46	1–115	16.61	0.33	0.66
47		15.20	0.24	0.58
48	1–116	14.49	—	0.39
49		17.78	0.40	0.76
50		17.36	0.54	0.97
51		16.91	0.38	0.81
52	1–106	15.93	0.37	0.69
53	1–90	16.70	0.35	0.68
54	1–89	15.42	0.20	0.38
55		19.20	0.69	1.65
56	1–25	15.38	0.21	0.44
57		18.61	0.38	0.92
58	1–109	15.79	0.31	0.68
59		15.32	0.24	0.52
60	1–77	15.80	0.21	0.50
61		16.91	0.30	0.76
62		16.31	0.63	1.15
63	1–82	16.06	0.20	0.47
64	1–83	16.01	0.62	1.21
65	1–84	16.38	0.33	0.68
66		14.62	—	0.58
67	1–26	14.44	—	1.05
68	1–70	16.01	0.25	0.52
69	1–74	14.98	0.16	0.34
70	1–75	15.46	—	1.12
71		17.24	0.14	0.23
72	1–27	14.38	—	0.27

Table 2. Continued.

Fig. 1(b) No.	TCW No.	V	V − R	V − I
73	1–29	16.10	0.30	0.60
74		17.64	0.44	0.87
75		17.50	0.33	0.81
76	1–67	14.92	0.11	0.28
77		18.42	0.49	1.03
78		17.01	0.47	0.98
79		18.79	0.59	1.16
80		17.39	0.40	0.81
81	1–32	14.47	—	0.27
82		18.70	0.79	1.48
83		18.21	0.44	1.22
84	1–66	15.95	0.30	0.56
85		18.57	0.31	0.94
86	1–65	15.85	0.24	0.46
87		19.95	1.04	2.05
88	1–62	15.91	0.24	0.64
89	1–33	14.12	—	0.48
90	1–64	15.23	—	1.13
91		17.78	0.66	0.97
92		16.84	0.62	1.30
93		17.50	0.48	1.07
94	1–50	14.57	—	0.48
Fig. 1(c) No.				
1	2–76	16.75	0.41	1.13
2	3–24	17.25	0.40	2.03
3		15.67	0.39	0.79
4		18.88	0.77	1.15
5		18.62	0.45	0.61
6		17.57	0.47	1.00
7		18.75	0.61	−0.50
8		18.90	0.74	1.41
9	2–79	16.63	0.59	1.14
10		19.33	1.18	2.00
11		19.01	0.71	1.39
12		17.06	0.42	0.84
13		16.97	0.32	0.75
14		17.10	0.34	0.67
15		18.40	0.64	1.50
16	2–80	16.18	0.51	1.00
17		18.98	0.88	1.59
18		17.96	0.49	0.70
19		19.21	0.81	1.39
20		18.67	0.36	0.97
21	1–57	16.45	0.40	0.69
22		18.37	0.66	1.32
23		18.35	0.48	0.73
24	2–74	15.80	0.23	0.50
25		16.73	0.28	0.76
26		17.73	0.23	0.66
27	2–73	16.60	0.68	1.26

Table 2. Continued.

Fig. 1(c) No.	TCW No.	V	$V-R$	$V-I$
28		16.68	0.36	0.69
29		18.43	0.65	1.23
30		17.89	0.34	−0.19
31		18.27	0.23	0.70
32		20.31	1.73	3.11
33		18.68	0.66	−0.03
34		18.59	0.57	1.29
35		17.90	0.47	0.92
36		18.12	0.47	0.88
37		16.84	0.31	0.22
38		16.74	0.39	0.98
39		17.13	0.44	0.91
40		17.58	0.90	1.72
41		17.66	0.50	1.23
42		17.44	0.47	1.07
43		18.48	0.47	0.78
44		18.88	0.98	1.80
45		17.89	0.47	0.85
46		18.81	0.63	1.67
47		17.74	0.42	0.72
48	2–66	16.23	0.32	0.66
49		18.18	0.43	0.64
50		18.97	0.38	1.20
51		18.08	0.49	0.85
52		19.00	1.06	2.15
53		18.33	0.61	1.27
54		18.35	0.43	0.68
55		18.57	0.62	1.34
56		17.17	0.20	0.56
57	1–80	15.37	0.17	0.37
58		18.07	0.42	0.67
59		16.70	0.26	0.75
60	2–60	16.24	0.34	0.73
61		17.34	0.73	1.39
62		18.57	0.41	0.93
63		16.91	0.13	1.03
64		18.10	0.51	1.25
65		18.36	0.64	1.17
66		17.54	1.53	0.75
67		18.90	1.31	1.08
68		15.69	0.26	0.50
69		17.99	0.47	0.67
70		18.55	0.27	1.07

$\pm$ 0.02 magnitude in V and B–V. As can be seen from Fig. 2, there seems to be a systematic difference in the values of V_{CCD} and V_{TCW} In the magnitude range 14 to 15.8 a constant difference of $-$ 0.08 (*i.e.* V_{CCD} is brighter) exists and between 15.8 and 16.8 the difference continuously increases from -0.08 to $+0.19$ magnitude. We compared the V magnitude of four common photoelectric standards measured by TCW which lie

in the V range of 15.4 to 16.86. The mean difference of V_{CCD} and V_{TCW} is $-$ 0.01. (Moreover our CCD standards are from $V = 15.9$ to 18.3.) Further, (a) CCD, unlike the photographic plate, is an intrinsically linear detector, and (b) in the present analysis magnitude estimation is based on the complex type profile which tackles not only crowding but also matches the star profile very closely. Therefore, we believe that magnitude estimation has been done in a relatively better way than TCW. So we conclude that the photographic V of TCW is affected by a systematic error which increases with magnitude for $V \geqslant 15.8$. Consequences of this systematic difference is mentioned in Section 4. One source of error in our photometry was employing the mean atmospheric extinction values. We expect the total error in $V - I$ to be $\simeq 0.06$ and in $V - R$ to be $\simeq 0.05$ mag.

3. **The colour-magnitude diagram (CMD)**

Fig. 3 shows the $V/(V - I)$ diagram for NGC 2818 for the central frame (centred on star 1–89 of TCW) in which field star contamination is expected to be minimal. Fig. 4 shows the same for all three fields (frames) combined. Since we were concentrating on the fainter stars, we did not have enough short exposures to include stars brighter than $V \sim 14$. So the sampling is rather restricted towards the brighter end. The spread in the colour around the cluster main-sequence seems to be little more than expected from
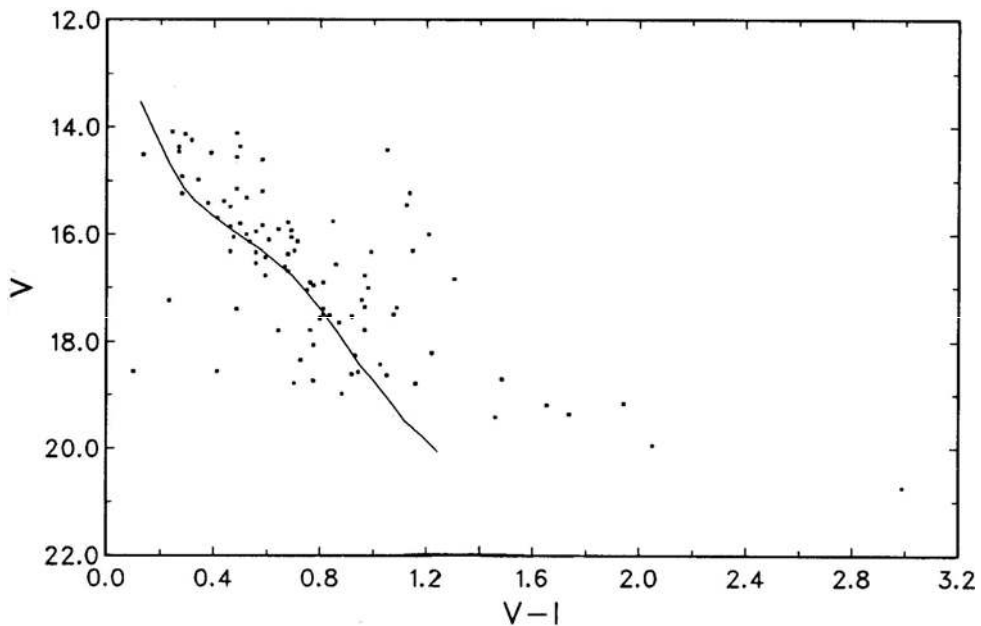
Figure 3. $V/V - I$ colour-magnitude diagram for the central frame covering 5×3 arcmin^2 around the cluster centre. The solid line corresponds to the ZAMS (Walker 1985) after applying reddening and interstellar extinction (A_V) corrections corresponding to $E(B - V) = 0.22$ for a distance modulus of $(m - M)_0 = 12.9$.
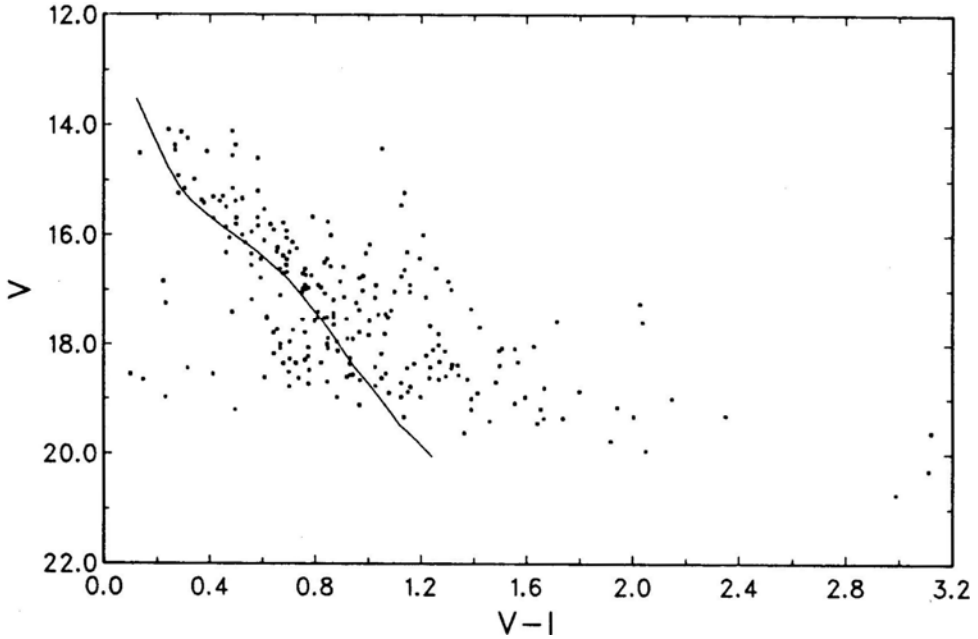
Figure 4. *V/V – I* colour–magnitude diagram of all the three fields observed. See caption to Fig. 3 for details.

the photometric errors alone. The *V/B – V* diagram of TCW also shows corresponding spread in the colour. Generally the spread in *V – I* colour is more than in *V – R* colour. As can be seen from Figs 3 and 4 the field star contamination increases for *V* > 17 and *V – I* > 0.7. However discrimination of the members and nonmembers based on *V – I* and *V – R* colours is not easy in practice.

3.1 *Reddening and ZAMS Fitting*

The mean cluster reddening was found by TCW from a (*U – B*), (*B – V*) plot as *E(B – V)* = 0.22. We adopt this value for the cluster reddening. Although *V – I* colour is more sensitive to reddening (*i.e.* $E(V – I) \simeq 1.25\, E(B – V)$], as pointed out by Walker (1985) and Romeo et al. (1989) due to slope of the reddening lines, *V – I* and *V – R* colours are not best suited for reddening determination. We adopt the reddening relation given by Dean, Warren & Cousins (1978) for estimating *E(V – I)* from *E(B – V)*:

$$E(V – I) = 1.25\, E(B – V)\, [1 + 0.06(B – V)_0 + 0.014\, E(B – V)],$$

and by Taylor (1986) for E(V - R):

$$E(V – R) = 0.59\, E(B – V).$$

The ratio of total to selective absorption R is expressed as a function of $(B – V)_0$ and *E(B – V)* by Walker (1985) and Romeo *et al.* (1989). We adopt the following expression

given by Romeo *et al.* (1989):

$$R = 3.06 + 0.25(B - V)_0 + 0.05\, E(B-V)$$

which is seen to be consistent with $R = 3.06$ for $(B - V) = 0.0$ and $E(B-V) = 0.0$, the galactic mean as determined by Turner (1976) from his extensive work on open clusters.

The zero age main sequence fitted to the cluster CMD is that given by Walker (1985) based on the Pleiades CMD. Fitting CM diagrams of young clusters to the Pleiades CMD also avoids the problem of applying controversial metallicity corrections. The examination of CM diagram of NGC 2818 (see further) indicates that the colour at which main sequence 'evolutionary' deviation from ZAMS occurs is at a spectral type of ~ A0–A1 which makes the cluster of comparable age to that of the Pleiades.

The location of the observed ZAMS in the CMD to an extent is a matter of taste, given the difficulty of discrimination between cluster members and nonmembers and the possible incidence of binaries. Thus, while fitting the ZAMS to the cluster we follow the theoretical definition which places it at the blue edge of the stellar distribution, once the photometric errors have been taken into account (*e.g.* Romeo *et al.* 1989).

We applied the reddening corrections to the ZAMS corresponding to $E(B - V)$ of 0.22 and using the above relation for $E(V - I)$ matched the ZAMS with the observed $V/(V—I)$ diagram as shown in Figs 3 and 4. The ZAMS can be fairly matched with $(m - M)_0$ of 12.9 ± 0.1. A similar value of the distance modulus is obtained from $V/(V - R)$ diagram; however, $V - R$ is less sensitive to the changes in the ZAMS fitting procedures. Based on the fit to the $V/(V - I)$ diagram we adopt $(m - M)_0 = 12.9$ which gives a distance of 3.8 kpc (or 3.66 kpc if $(m - M)_0 = 12.8$). This value is quite consistent with the estimate made by Dufour (1984) from an independent evaluation of the TCW data.

The above ZAMS fitting procedure assumes that the metal abundance is similar to the Pleiades (*i.e.* solar) and any deviation from this introduces uncertainty. The spread in the $V - I$ colour of the main sequence in the CMD is ~ 0.275 to 0.30 at $V = 16$ to $V = 17$ which in most part is intrinsic; as a comparison the Pleiades CMD also has a spread of 0.4 mag in $V - I$ at $V = 16$ (Stauffer 1984). This might be a result of several effects like the presence of binaries, spotted stars, rotation *etc.*; it could also have been a result of some variable extinction in the cluster stars but evaluation of this aspect would need colour excess estimates of individual stars across the cluster, which is not attempted here.

4. Discussion

Although the cluster sequence is well defined in our CM diagrams (Figs 3 and 4) the TCW CM diagrams indicate substantial foreground and background field star contamination. TCW mention a sequence of F to K dwarfs which show reddening less than the cluster. The group left of ZAMS and fainter than $V \sim 17$ present in Fig. 4 might correspond to this group.

TCW mention a break in the cluster main sequence at $V \sim 16.2$ (Fig. 2 of TCW) and also that the main sequence abruptly terminates at $V \sim 15.9$. They felt that the bend or break in the main sequence at $V \sim 15.9$ is probably real. But no such break can be seen in our CM diagram, and the similarity invoked with the break in the main sequence of

NGC 752 by TCW does not apply. TCW also mention that at this magnitude a redder group of stars appears and continues downward to the limit of photometry ($V \sim 16.8$). A similar 'displaced' configuration of stars appears in their intermediate and outer zones. This appears to be the result of the systematic error in V magnitude present in TCW's photographic photometry mentioned in Section 2.2. We have tried to study this further by supposing that only the V magnitudes of TCW had errors but not their B magnitudes. So for the common stars between these two studies we applied a correction to the $(B - V)$ of TCW by a value equal to the difference between V_{CCD} and V_{TCW} and plotted a colour-magnitude diagram for these stars with V_{CCD} versus corrected $B - V$ of TCW. No break in the sequence is found at $V \sim 16.2$; and moreover this is consistent with $(m - M)_0$ of 12.9 when the ZAMS (Walker 1985) was superposed on this CMD (Fig. 5) confirming that the photometric errors are responsible for the break in TCW's CMD at $V \sim 162$.

The turnoff spectral type from the ZAMS is estimated by TCW based on their $B - V$ colour as A5. $((B - V)_0 = 0.15 \pm 0.04)$. This is not consistent with the observations presented here. The zero age main sequence turnoff seems to occur at $V \sim 15.3$ and $(V - I)_0 = 0.04 \pm 0.03$ corresponding to a spectral type of $\sim$ A1.5 (Bessell 1979) which would make the cluster younger than estimated by TCW.

4.1 *Association with the* PN

The association of the PN and the cluster has been discussed by Dufour (1984). The PN is a prototype of Type I nebulae with helium and nitrogen being abundant. It also
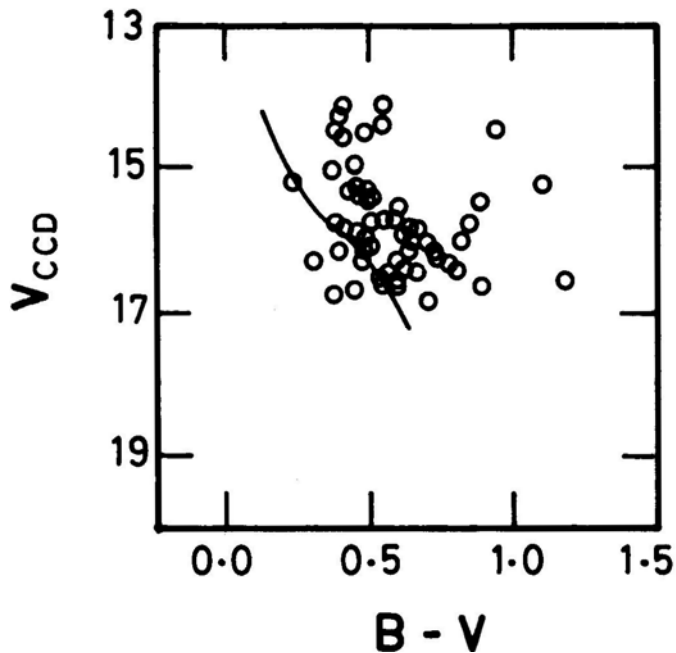

Figure 5. $V_{CCD}/(B–V)_{TCW}$ diagram for stars in common with TCW. A systematic correction to $B - V$ equal to the difference between V_{CCD} and V_{TCW} (Fig. 2) has been applied. The continuous line is the ZAMS as in fig. 3.

seems to be a bipolar nebula (Louise *et al.* 1987). Since the present investigation gives the same distance as that estimated by Dufour, there are no major changes to his derived parameters of the PN. However, the change of the turnoff spectral type of Al would increase the estimated PN progenitor mass. A comparison of our $V/(V - I)$ CMD with the isochrones computed by van den Berg (1985) (*i.e.* his tabulated M_v, $V - I$) for stars in the mass range of 1 to $3M_\odot$ and the solar metallicity indicates an age of $5 \pm 1 \times 10^8$ years to the cluster. And the progenitor mass of the PN would be greater than $\geq 2.58\ M_\odot$ if the cluster age is 5×10^8 years ($>2.45\ M_\odot$ if $\sim 6 \times 10^8$ years). Good agreement of the radial velocity as well as $E(B - V)$ value of the PN with those of the cluster strongly support the association of the cluster and the PN. Since the independent estimates of PN distances are statistical in nature, the larger values of distance obtained for the cluster need not be looked upon as a discrepancy. If the estimated distance of 3.8 kpc for the cluster is taken as the distance of the PN also (this value is also consistent with a kinematical distance estimated from the galactic rotation: Dufour 1984), then, the central star parameters as given by case B of Kohoutek, Roth-Hopper, Laustsen (1986) apply *i.e.* $L_*/L_\odot \sim 103$, $R_* \simeq 0.04\ R_\odot$, the nebular hydrogen mass $\sim 0.25\ M_\odot$ and $M_v \simeq 5$.

5. Conclusions

The CCD photometry of the cluster in *VRI* bands down to $V \sim 20$ mag, presents a well-defined ZAMS of the cluster. The fitting of the ZAMS applicable to the Pleiades (Walker 1985) with the $V/(V - I)$ CMD of NGC 2818 gives a distance modulus ($m - M)_0 = 12.9$ and a distance of 3.8 kpc for the cluster. Applying van der Berg's (1985) theoretical isochrones computed with solar metallicity indicates an age $\sim 5 \times 10^8$ years. If the PN is taken to be belonging to the cluster (which is likely) then the progenitor star mass must be $\geq 2.5M_\odot$. Further observations of this cluster are planned in order to study the brighter members and the nebula.

Acknowledgements

References

Ananth, A. V., Srinivasan, R., Srinivasulu, G., Chandramouli, S. S., Chinnappan, V. 1989, *VBT News,* No. 1.

Bessell, M. S. 1979, *Publ. astr. Soc. Pacific,* **91**, 589.

Christian, C. A., Adams, M., Barnes, J. V., Butcher, H., Hayes, D. S., Mould, J. R., Spiegel, M. 1985, *Publ. astr. Soc. Pacific,* **97**, 363.

Dean, J. F., Warren, P. R., Cousins, A. W. J. 1978, *Mon. Not. R. astr. Soc.*, **183**, 569.

Dufour, R. J. 1984, *Astrophys. J.,* **287,** 341.
Kohoutek, L., Roth-Hopper, M. L., Laustsen, S. 1986, *Astr. Astrophys.,* **162**, 232.
Louise, R., Macron, A., Pascoli, G., Maurice, E. 1987, *Astr. Astrophys. Suppl.,* **70**, 201.
Penny, A. J., Dickens, R. J. 1986, *Mon. Not. R. astr. Soc.,* **220**, 845.
Penny, A. J. 1987, *Space Teles. Sci. Inst. Rep.*
Romeo, G., Bonifazi, A., Fusi Pecci, F., Tosi, M. 1989, *Mon. Not. R. astr. Soc.,* **240**, 459.
Stauffer, J. R. 1984, *Astrophys. J.,* **280**, 189.
Taylor, B. J. 1986, *Astrophys. J. Suppl. Ser.,* **60**, 577.
Tifft, W. G., Connolly, L. P., Webb, D. F. 1972, *Mon. Not. R. astr. Soc,* **158**, 47 (TCW).
Turner, D. G. 1976, *Astr. J.,* **81**, 1125.
van den Berg, D. A. 1985, *Astrophys. J. Suppl.,* **58**, 711.
Walker, A. R. 1985, *Mon. Not. R. astr. Soc.,* **213**, 889.

Note added in proof

After this paper went to press we became aware of the work of Pedreros (*Astr. J.* 1989 **98,** 2146.) on this cluster. He derives a distance modulus which is smaller by a magnitude. Pedreros' photometry is on TCW system which according to us, has a systematic error for stars fainter than $V = 15.8$. He adapts [Fe/H] value of -0.34 and compares his CM diagram with theoretical isochrones of van den Berg. We assumed solar metallicity based on the work of Dufour on the metallicity of PN (particularly sulphur) and we used the observational ZAMS of Walker to fit the cluster main sequence. Independent determination of the metallicity of the cluster is needed.